Journal of Engineering Mathematics, Vol. 7, No. 4, October 1973
Noordhoff International Publishing–Leyden
Printed in The Netherlands

Shear flow past a flat plate

V. O. S. OLUNLOYO

Department of Theoretical and Applied Mechanics, Cornell University, Ithaca, N. Y., U.S.A.

(Received September 5, 1972)

SUMMARY

The controversy over the induced pressure gradient in shear flow is re-examined in the context of general bounding. It is shown that the results reported by Ludford and this author in two earlier papers are indeed typical near the leading edge. However far downstream they are only valid in the presence of walls. In particular two new effects arise; for weak bounding logarithmic terms appear in the inviscid pressure and a resonance with the first eigensolution occurs. For the symmetric case Toomre and Rott's result is recovered.

1. Introduction

The controversy over the boundary layer on a flat plate in shear flow originally started by Li [1] has received the attention of several authors. Suffice it to say that from the beginning there were two separate, even though sometimes confused, issues involved. The first concerned the existence of an induced pressure gradient outside the boundary layer. Such a pressure gradient has fundamental significance because a modified pressure field consequently affects the skin friction, the heat transfer, boundary layer separation and the laminar stability characteristics of the flow. This question was affirmatively answered when Murray [2], by careful matching showed that the revised solution given by Li was correct for the purely mathematical problem of unbounded shear flow.

However Glauert's [3] second criticism remained unanswered; namely whether Murray's solution played any significant role in realistic situations where the incident shear flow is necessarily bounded. Later Toomre and Rott [4] attempted to resolve the issue by actually determining the disturbance to the inviscid flow due to the first order (Blasius) boundary layer for a bounded shear flow U_0+Ay for $|y|\leqq h$ and U_0+Ah for $|y|\geqq h$, the plate lying along the positive x-axis. Their main result was that the Li–Murray pressure gradient is accurate in only a very limited region near the leading edge. This seemed to resolve the remaining question and Van Dyke in a recent account of the controversy [5] effectively declared the matter closed.

This proved premature in view of criticisms raised by Koch *et al.* [6] while addressing themselves to a different question. They questioned the practicality of the profile used by Toomre and Rott. Kinks, such as the one at $y=0$ in their case make their profile unrealistic and its symmetry rules out certain key effects *a priori.*

Accordingly, Ludford and Olunloyo [7] returned to the Couette profile introduced by Glauert (who only gave it an *ad hoc* treatment), namely U_0+Ay for $|y|<h$, the walls at $y=\pm h$ moving with the fluid. Their conclusion was that the Li–Murray solution for unbounded shear flow does not play the main role for the bounded shear they considered. They showed that the induced global circulation predicted by Glauert does in fact occur contributing an $O(x^{\frac{1}{2}})$ term to the leading edge lift being more important than Li–Murray's $O(x^{\frac{3}{2}})$. Furthermore in this neighborhood, the leading term for the drag is provided not by Li–Murray but by the bounding it being $O(x^{\frac{1}{2}})$ compared with Li–Murray's $O(x)$. By setting the plate off the axis of the channel it was further shown [8] that local circulation could be induced around the leading edge of the plate by the walls bounding the shear. Such a local circulation gives an $O(x^{\frac{1}{2}})$ lift in this region while the resulting distortion of the induced global circulation now provides

$O(x^{\frac{1}{2}})$ drag. Based on their analysis it was then predicted that no new effects could arise from other forms of bounding.

Such a generalization would not be suspect were it true that shear flows as met in practice are always bounded by walls. In fact two forms of bounding are generally used for finite shear and Goldstein in his review article [9] proposed replacing Murray's linear shear profile with one which levels off far away from the plate on either side into a uniform flow; this being a weaker form of bounding than that proposed by Glauert. [By weak bounding it is implied that not more than one wall is used in limiting the shear. For strong bounding the shear must be restricted on both sides by walls.] One essential difference between the two is that for strong bounding (i.e. the latter), the disturbance streamfunction is independent of the shear (see [7] for example) whereas for weaker forms of bounding it is a function of the shear (*cf.* [4]). For completeness, it is essential to confirm these predictions under a more general form of bounding.

We therefore look for a model that incorporates both forms of bounding found in practice. In the present study the shear flow $U_0 + Ay$ is restricted to the region $-ah \leqq y \leqq h$ being limited by a wall moving with the fluid at $y = h$ and by a uniform flow at $y = -ah$ (Fig. 1) where $h \gg 1$ but finite. Note that this is not a serious limitation since as pointed out in [7] the effects we are interested in will always persist, if present, even when the bounding recedes to infinity. The plate has been displaced off the centerline to incorporate effects of asymmetry in the bounding. A straight forward attack leads to what appears to be an intractable Wiener–Hopf equation. Instead an asymptotic solution is constructed from superposition of two more fundamental problems each of which admits exact solution through the Wiener–Hopf technique.

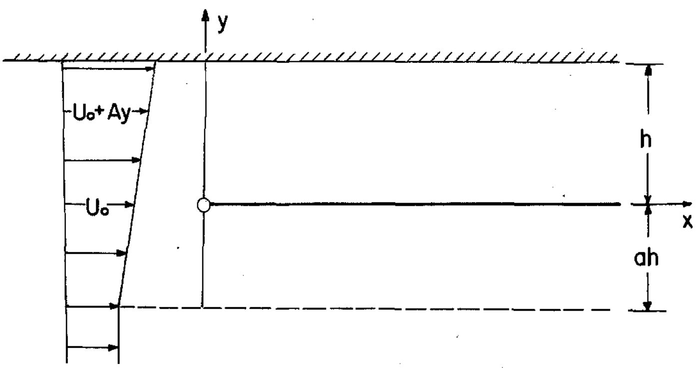

Figure 1. Flow geometry.

Near the leading edge the effects predicted in [7] are confirmed. However local circulation can now be induced, even in the symmetric case, by arranging different forms of bounding on either side of the plate.

On the other hand, the behavior far downstream on either side of the plate is strongly influenced by the type of bounding seen by that side of the plate. For the case of symmetric bounding the pressure gradient below the plate becomes a vanishingly small multiple of the Li–Murray value, confirming Toomre and Rott's result while on top of the plate, the result in [7] is recovered. For our case we find that the asymptotic series for the inviscid surface speed above the plate starts with an $x^{\frac{1}{2}}$ term and decreases in powers of x the next term being $O(x^{-\frac{1}{2}})$, and so on. Below the plate the surface speed decays like $x^{-\frac{3}{2}}$ followed by inverse powers of x; in addition log terms like $x^{-3} \log x$ for the first time appear. Such log terms induce, through matching, corresponding terms in the boundary layer.

In general, the pressures would be different on both sides of the plate (even for the same type of bounding provided there is asymmetry) and an induced global circulation is set up on equalizing pressures at a station on the plate far downstream. Such an induced global circulation is considered here. Far downstream the asymptotic expansion for the inviscid speed is a constant above the plate; below the plate it starts off with x^{-1} followed by terms like $x^{-2} \log x$ and inverse powers of x. The forcing function associated with the leading term (below the plate) is $x^{-\frac{1}{2}}$ and because its exponent $(-\frac{1}{2})$ coincides with the first eigenvalue for the eigensolutions in the boundary layer (*cf.* Libby and Fox [10]), a curious resonance occurs. Such a resonance which is independent of the shear can be simulated whenever the flow is weakly bounded (including Li–Murray case) by terminating the plate far downstream and pumping the recombined streamlines further downstream.

Above the plate no such effect is found and it is clear that such resonance was suppressed in [7] and [8] by the presence of walls; it is also missing in Toomre and Rott's case because the dynamic symmetry of their profile rules out induced circulations.

2. Formulation of the boundary value problem

The problem is to find an inviscid flow field satisfying

$$\begin{aligned} &v(x, \pm 0) = \pm C x^{-\frac{1}{2}} \text{ for } x>0; \quad v(x,h)=0 \text{ for all } x\,, \\ &v(x,y) \to 0 \text{ as } y \to -\infty \end{aligned} \tag{2.1}$$

and tending far upstream to the shear flow bounded by the uniform stream (*cf.* Fig. 1). Here the small constant

$$C = \tfrac{1}{2}\beta (U_0 \nu)^{\frac{1}{2}}\,, \quad \beta = 1.7208$$

comes from the Blasius solution for the boundary layer. In addition to the forementioned boundary conditions we must enforce the physical requirement that (a) the normal velocity v and (b) the streamwise pressure gradient be continuous across the interface separating the shear and the potential flow regions. As pointed out by Toomre and Rott, such matching should be carried out at the (unknown) displaced location of the interface boundary; but under the presumption that the disturbance is infinitesimal (*cf.* [4]) the matching can be carried out along the line $y=-ah$.

We introduce a disturbance streamfunction ψ, so that the velocity components are

$$u = U_0 + Ay + \psi_y\,; \quad v = -\psi_x\,.$$

Since the vorticity in the disturbed flow remains constant at $-A$, the function ψ satisfies Laplace's equation with the boundary values

$$\psi(x,h) = 0\,, \tag{2.2a}$$

$$\psi(x,\pm 0) = \begin{cases} Ch^{\frac{1}{2}} g(x) & \text{for } x<0\,, \\ \mp 2Cx^{\frac{1}{2}} + \psi_0 & \text{for } x>0\,, \end{cases} \tag{2.2b}$$

and

$$\Delta\psi_y(x,0) = \begin{cases} 0 & \text{for } x<0\,, \\ Ch^{\frac{1}{2}} f(x) & \text{for } x>0\,. \end{cases} \tag{2.2c}$$

We have hereby introduced two unknown functions $f(x)$ and $g(x)$ on the positive and negative x-axis respectively; the integration constant ψ_0 added for $x>0$ in condition (2.2b) corresponds to the addition of a (global) circulation around the plate.

To determine ψ we can take a Fourier transform of the governing equation and the appropriate boundary values but because the boundary conditions on $y=0$ are mixed this leads to a Wiener–Hopf problem which in this case appears intractable.

Alternatively we can write the total streamfunction as

$$\Psi = \Psi^* + \Psi^c = \tilde{\alpha}\Psi_{\mathrm{I}} + \tilde{\beta}\Psi_{\mathrm{II}} + \Psi^c \tag{2.3}$$

where $\tilde{\alpha}$ and $\tilde{\beta}$ are scalars to be determined and where Ψ^c representing the second order global circulation satisfies the boundary conditions (2.1) with $C=0$. Like Ψ^c, Ψ_{I} and Ψ_{II} satisfy Laplace's equation and in fact

$$\Psi_{\mathrm{I}} = U_0 y + \tfrac{1}{2} A_1 y^2 + \psi_1 \tag{2.4}$$

is the total streamfunction for the profile shown in Fig. 2.

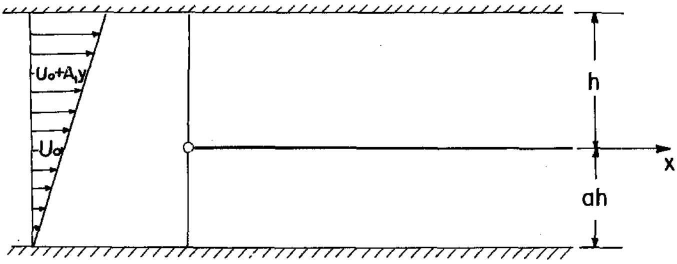

Figure 2.

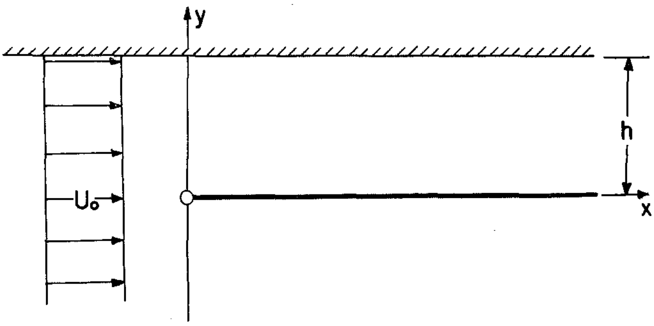

Figure 3.

For this problem it is easily verified that ψ_1 satisfies Laplace's equation and the boundary values (2.2) with $\psi_0=0$. In addition we have

$$\psi_1(x, -ah)=0 \text{ for all } x\,. \tag{2.5}$$

On the other hand we can also write

$$\Psi_{\text{II}}= U_0 y+\psi_2 \tag{2.6}$$

as the streamfunction for the profile described by Fig. 3. Here again ψ_2 is a harmonic function satisfying the boundary conditions (2.2) with $\psi_0=0$, and decays to zero as $y\to-\infty$.

Problems for ψ_1 and ψ_2 are special cases of the general problem treated by Ludford and Olunloyo [8]. ψ_1 can, for example, be evaluated by putting $A=U_0/ah$ into their result for the disturbance streamfunction. Moreover since their disturbance streamfunction is independent of the shear ψ_2 then corresponds to their ψ in the limit of their lower wall receding to $y=-\infty$. However while ψ_2 may be a special case of their problem its value cannot be easily deduced from their results. Indeed it has enough peculiar difficulties to warrant special attention. [ψ_2 also arises in a recent treatment of the inlet problem by Kapila, Ludford and Olunloyo [11].]

Thus we proceed to construct the solution to the profile in Fig. 1, by taking a linear combination of the two special cases discussed above. For such a superposition we must ensure that all necessary boundary conditions are preserved and the vorticity in the disturbed flow must remain constant at $-A$.

This latter condition demands that $A=\tilde{\alpha}A_1=\tilde{\alpha}U_0/ah$, while the former gives $\tilde{\alpha}+\tilde{\beta}=1$. Hence

$$\tilde{\alpha}= A/A_1 = Aah/U_0\,;\quad \tilde{\beta}= 1-Aah/U_0\,. \tag{2.7}$$

Note that continuity of the normal velocity along the line $y=-ah$ in Fig. 1 is guaranteed by the fact that it vanishes identically everywhere along the lower wall in the problem for Ψ_{I}. The pressure condition is also asymptotically satisfied everywhere along the line provided $h\gg 1$. When $h=O(1)$ this condition is still satisfied far upstream and downstream on the line $y=-ah$ but it is now violated near the y axis. It can however be easily shown that even for this case the results presented here are still asymptotically valid except near the leading edge where the computed coefficients can now only be regarded as estimates even though it is clear that no new effects arise there.

The Fourier transform is defined as

$$\bar{\psi}(y,\xi)=\int_{-\infty}^{\infty}\psi(x,y)e^{-i\xi x}dx\,,$$

with the inverse

$$\psi(x,y)=\frac{1}{2\pi}\int_{-\infty}^{\infty}\bar{\psi}(y,\xi)e^{i\xi x}d\xi$$

where the need for an indentation below the origin will be clear as we proceed.

If we rewrite Ψ^* as $\Psi^*=\psi^*+\psi^{**}$

where

$$\psi^*=\begin{cases}U_0+Ay & \text{for}\quad -ah\leqq y\leqq h\,,\\ U_0-Aah & \text{for}\quad y\leqq ah\,,\end{cases}\tag{2.8}$$

then

$$\frac{\psi^{**}}{Ch^{\frac{1}{2}}}=\begin{cases}(\tilde{\alpha}\bar{g}_{1\oplus}+\tilde{\beta}\bar{g}_{2\oplus}-\bar{n}_{\ominus})\dfrac{\sinh\xi(h-y)}{\sinh\xi h} & \text{for}\quad 0\leqq y\leqq h\,, \qquad (2.9\text{a})\\ \tilde{\alpha}(\bar{g}_{1\oplus}+\bar{n}_{\ominus})\dfrac{\sinh\xi(ah+y)}{\sinh a\xi h}+\tilde{\beta}(\bar{g}_{2\oplus}+\bar{n}_{\ominus})e^{|\xi|y} & \text{for}\quad -ah\leqq y\leqq 0\,, \qquad (2.9\text{b})\\ \tilde{\beta}(\bar{g}_{2\oplus}+\bar{n}_{\ominus})e^{|\xi|y} & \text{for}\quad y\leqq ah \qquad (2.9\text{c})\end{cases}$$

satisfying the boundary conditions (2.2a, b) with $\psi_0=0$. Here

$$\bar{n}_{\ominus}=h^{-\frac{1}{2}}\pi^{\frac{1}{2}}(i\xi)^{-\frac{3}{2}}$$

corresponding to

$$n(x)=\begin{cases}0 & \text{for}\quad x<0\,,\\ 2h^{-\frac{1}{2}}x^{\frac{1}{2}} & \text{for}\quad x>0\,.\end{cases}$$

$\bar{g}_{1\oplus}$ and $\bar{g}_{2\oplus}$ are the transforms of the disturbance stream functions ψ_1 and ψ_2 respectively on the negative x-axis. They are found by solving the corresponding Wiener–Hopf equations for $\bar{\psi}_1$ and $\bar{\psi}_2$. Details of the procedure can be found in [8] or [11] and is illustrated in Section 5 where the induced global circulation is treated.

To be more precise

$$\bar{g}_{1\oplus}=\frac{P_{1\oplus}}{K_{1\oplus}}\,;\quad \bar{g}_{2\oplus}=\frac{P_{2\oplus}}{K_{2\oplus}}\tag{2.10}$$

where

$$P_{1\oplus}(\xi)=\frac{h}{2\pi i}\int_{-\infty}^{\infty}\frac{z\sinh z(1-a)h\bar{n}_{\ominus}(z)}{K_{1\ominus}(z)\sinh zh\sinh azh}\frac{dz}{z-\xi}\,,\tag{2.11}$$

$$K_{1\oplus}(\xi)=-\frac{\Gamma\left(1-\dfrac{i\xi h}{\pi}\right)\Gamma\left(1-\dfrac{i\xi ah}{\pi}\right)}{\Gamma\left(1-\dfrac{i\xi(1+a)h}{\pi}\right)}\times\exp\left\{\left(\frac{ai\xi h}{\pi}-\frac{1}{2}\right)\ln a+\left(\frac{1}{2}-\frac{i\xi h}{\pi}-\frac{ai\xi h}{\pi}\right)\ln(1+a)\right\}\,,\tag{2.12}$$

$$K_{1\ominus}(\xi)=\frac{i\xi h}{\pi}\frac{\Gamma\left(\dfrac{i\xi h}{\pi}\right)\Gamma\left(\dfrac{i\xi ah}{\pi}\right)}{\Gamma\left(\dfrac{i\xi(1+a)h}{\pi}\right)}\exp\left\{\left(\frac{1}{2}-\frac{ai\xi h}{\pi}\right)\ln a-\left(\frac{1}{2}-\frac{i\xi h}{\pi}-\frac{ai\xi h}{\pi}\right)\ln(1+a)\right\}\,,\tag{2.13}$$

and where

$$P_{2\oplus}(\xi) = \frac{h}{2\pi i} \oint_{-\infty}^{\infty} \frac{\bar{n}_{\ominus}(z)|z|(\coth|z|h-1)}{K_{2\ominus}(z)(z-\xi)}\, dz \tag{2.14}$$

with

$$K_{2\ominus}(\xi) = \Gamma\left(1+\frac{i\xi h}{\pi}\right) \times \exp\left\{\frac{|\xi|h}{\pi}\left(\frac{\pi}{2} - i\log\left(\frac{|\xi|+\xi}{\varepsilon}\right)h\right) + \frac{i\xi h}{\pi}\left(1-\log\frac{\varepsilon}{2\pi}\right)\right\} \tag{2.15}$$

and

$$K_{2\oplus}(\xi) = \Gamma\left(1-\frac{i\xi h}{\pi}\right) \times \exp\left\{\frac{|\xi|h}{\pi}\left(\frac{\pi}{2} + i\log\left(\frac{|\xi|+\xi}{\varepsilon}\right)h\right) - \frac{i\xi h}{\pi}\left(1-\log\frac{\varepsilon}{2\pi}\right)\right\}. \tag{2.16}$$

The lower subscript $\oplus$ denotes a function of ξ that is regular in an upper half plane $\text{Im}\,\xi > \tilde{a}$, while the lower subscript $\ominus$ denotes a function regular in a lower half plane $\text{Im}\,\xi < \tilde{b}$. The Wiener–Hopf method requires that these two half-planes overlap, i.e. $\tilde{b} > \tilde{a}$. For functions with upper subscript 1, the strip of regularity is $-\pi/(1+a)h < \text{Im}\,\xi < 0$, while those with upper subscript 2 have their strip of regularity at $-\varepsilon/h < \text{Im}\,\xi < 0$. As in all Laplace equation problems, in order to guarantee an overlap strip we must treat $|\xi|$ as the limit

$$\lim_{\varepsilon\to 0} (\xi^2 + \varepsilon^2/h^2)^{\frac{1}{2}}$$

the cuts being $(-i\infty, -i\varepsilon/h)$ and $(i\varepsilon/h, i\infty)$ so that the inversion line (which must lie within the strip of regularity) is indented below the origin in the complex ξ-plane. Finally, in the formulas (2.15) and (2.16) the branch cuts for the log are chosen so that for $K_{2\ominus}$ the expression $\pi/2 - i\log((|\xi|+\xi)h/\varepsilon)$ is zero at $\xi = -i\varepsilon/h$ while for $K_{2\oplus}$ the expression $\pi/2 + i\log((|\xi|+\xi)h/\varepsilon)$ is zero at $\xi = i\varepsilon/h$.

We also note here that it is clear from (2.9) that our disturbance streamfunction will in general be a function of the shear A.

3. Calculation of the pressure

When quadratic terms in ψ are neglected, the x-momentum equation integrates to give

$$p = -\rho(U_0 + Ay)(\tilde{\alpha}\psi_{1y} + \tilde{\beta}\psi_{2y}) + \rho A(\tilde{\alpha}\psi_1 + \tilde{\beta}\psi_2)$$

so that on the x-axis

$$p(x, \pm 0) = -\rho U_0[\tilde{\alpha}\psi_{1y}(x, \pm 0) + \tilde{\beta}\psi_{2y}(x, \pm 0)] + \rho A[\tilde{\alpha}\psi_1(x, \pm 0) + \tilde{\beta}\psi_2(x, \pm 0)]. \tag{3.1}$$

It is convenient to write

$$p = p^{\infty} + p^r + p^l$$

where

$$p^{\infty} = \tfrac{1}{2}(1-\text{sgn}\,x)\rho U_0 C|x|^{-\frac{1}{2}} \mp (1+\text{sgn}\,x)\rho A C x^{\frac{1}{2}} \tag{3.2}$$

is the pressure in an unbounded flow without circulation (Li–Murray), and

$$p^r(x, \pm 0) = \begin{cases} -2\rho U_0 C \displaystyle\int_{-\infty}^{\infty} [\pi^{-1}\tilde{x}^{-2} - \tfrac{1}{4}\pi h^{-2}\,\text{cosech}^2(\tfrac{1}{2}\pi h^{-1}\tilde{x})](x-\tilde{x})^{\frac{1}{2}}\, d\tilde{x}\,, & (3.3a) \\ -2\rho C A a h \displaystyle\int_{-\infty}^{\infty} [\pi^{-1}\tilde{x}^{-2} - \tfrac{1}{4}\pi a^{-2} h^{-2}\,\text{cosech}^2(\tfrac{1}{2}\pi a^{-1} h^{-1}\tilde{x})](x-\tilde{x})^{\frac{1}{2}}\, d\tilde{x}\,, & (3.3b) \end{cases}$$

and

$$p^l(x,\pm 0)=\begin{cases} \tfrac{1}{2}(1-\operatorname{sgn} x)\rho ACU_0^{-1}h^{\frac{1}{2}}\left[Aah(g_1(x)-g_2(x))+U_0 g_2(x)\right] \\ \quad +\dfrac{\rho CAah^{\frac{1}{2}}}{2\pi}\displaystyle\oint_{-\infty}^{\infty}\bar{g}_{1\oplus}h\xi\coth\xi h\, e^{i\xi x}d\xi \\ \quad +\dfrac{\rho Ch^{\frac{1}{2}}}{2\pi}(U_0-Aah)\displaystyle\oint_{-\infty}^{\infty}\bar{g}_{2\oplus}\xi\coth\xi h\, e^{i\xi x}d\xi\,, & (3.4a) \\ \tfrac{1}{2}(1-\operatorname{sgn} x)\rho ACU_0^{-1}h^{\frac{1}{2}}\left[Aah(g_1(x)-g_2(x))+U_0 g_2(x)\right] \\ \quad -\dfrac{\rho CAah^{\frac{1}{2}}}{2\pi}\displaystyle\oint_{-\infty}^{\infty}\bar{g}_{1\oplus}h\xi\coth a\xi h\, e^{i\xi x}d\xi \\ \quad -\dfrac{\rho Ch^{\frac{1}{2}}}{2\pi}(U_0-Aah)\displaystyle\oint_{-\infty}^{\infty}\bar{g}_{2\oplus}|\xi|\, e^{i\xi x}d\xi & (3.4b) \end{cases}$$

are corrections due to the bounding. The derivation of p^∞ and p^r is analogous to that for p^∞ and p^w in [7] while the derivation for p^l is similar to that for p^l in [8]. It is obvious that p^r is the pressure when the dividing streamline ahead of the plate is held *rigidly* along the negative x-axis. For the case treated in [8], where the bounding was by walls on both sides, it was noted that p^r was independent of the shear but instead depended on the location of the walls. Here we find that while the pressure on the side of the plate facing the wall confirms this, the pressure below the plate depends not only on the location of the other bounding but also on the shear. The fact that the discontinuity in p^r is preserved even in the symmetric case ($a=1$) reflects this dependence on shear; in fact such dependence on shear persists whenever the shear flow is weakly bounded. As expected, in the limit $Aah\to U_0$, the results obtained for p^r here coincide with those presented in [8] since in this limit there is essentially no difference in the two bounded profiles as seen by the plate.

The discontinuity in p^r across the x-axis is in all cases, cancelled along the negative x-axis by p^l. The latter corresponds to a *local* circulation around the plate in which the dividing streamline is displaced and, in particular, attaches behind the leading edge. It is clear from (3.4) that asymmetric bounding is a sufficient condition for inducing local circulation. Its existence does not depend on the use of walls and would still be present if our wall (Fig. 1) is replaced by a uniform stream moving at the corresponding velocity provided $a\neq 1$.

Our primary interest lies in the comparative behaviors of these three pressures along the plate and its extension upstream.

4. Distribution of pressure along the x-axis

The expansion for p^∞ near the leading edge can be obtained directly but for p^r and p^l it is better to use the Fourier transforms

$$\bar{p}^r(\xi,\pm 0)=\begin{cases} -\rho U_0 Ch^{\frac{1}{2}}\bar{n}_\ominus|\xi|(\coth|\xi|h-1)\,, & (4.1a) \\ -\tilde{\alpha}\rho U_0 Ch^{\frac{1}{2}}\bar{n}_\ominus|\xi|(\coth a|\xi|h-1)\,, & (4.1b) \end{cases}$$

$$\bar{p}^l(\xi,\pm 0)=\rho ACh^{\frac{1}{2}}(\tilde{\alpha}\bar{g}_{1\oplus}+\tilde{\beta}\bar{g}_{2\oplus})+\begin{cases} \rho U_0 Ch^{\frac{1}{2}}(\tilde{\alpha}\bar{g}_{1\oplus}+\tilde{\beta}\bar{g}_{2\oplus})|\xi|\coth|\xi|h\,, & (4.2a) \\ -\rho U_0 Ch^{\frac{1}{2}}(\tilde{\alpha}\bar{g}_{1\oplus}\coth a|\xi|h+\tilde{\beta}\bar{g}_{2\oplus})|\xi|\,. & (4.2b) \end{cases}$$

The transforms must each be decomposed into functions regular in half planes. The asymptotic expansions of these functions as $\xi\to\infty$ then give the required behavior. We can for example write

$$\bar{n}_\ominus|\xi|(\coth|\xi|h-1)=F_\oplus+F_\ominus$$

where by the decomposition theorem (see Noble [12, p. 13])

$$F_{\oplus} = \pm \frac{1}{2\pi i} \oint \frac{\bar{n}_{\ominus}(z)\,|z|\,(\coth|z|h-1)}{z-\xi}\,dz\,.$$

Because of the exponential convergence at $z=\pm\infty$, the asymptotic expansion of $F_{\pm}$ can be obtained by writing

$$(z-\xi)^{-1} = -(1+z/\xi+z^2/\xi^2+\ldots)/\xi$$

in its integrand and integrating term by term. Thus as $\xi\rightarrow\infty$

$$F_{\oplus} = \mp \frac{1}{i\xi h}\left\{a_0 + \frac{a_1}{h\xi} + \frac{a_2}{(h\xi)^2} + \ldots\right\} \tag{4.3}$$

where the coefficients

$$a_n = \frac{h^{n+1}}{2\pi} \lim_{\varepsilon\rightarrow 0} \int_{-\infty}^{\infty} \bar{n}_{\ominus}(z)|z|\,z^n(\coth|z|h-1)dz \tag{4.4}$$

are independent of h and can be shown to be related to the Riemann ζ functions. Thus

$$p^r(x,+0) = \rho U_0 C h^{\frac{1}{2}}[a_0+a_1(x/h)+O(x^2/h^2)] \text{ as } x\rightarrow\pm 0\,, \tag{4.5a}$$

$$p^r(x,-0) = \rho C A a^{\frac{1}{2}} h^{\frac{3}{2}}[a_0+a_1(x/ah)+O(x^2/a^2h)] \text{ as } x\rightarrow\pm 0 \tag{4.5b}$$

where

$$a_0 = \zeta(\tfrac{1}{2}) = -1.460\;;\;\; a_1 = -\tfrac{1}{4}\zeta(\tfrac{3}{2}) = -0.653\,.$$

In dealing with $\bar{p}^l$, asymptotic behavior of $\bar{g}_{1\oplus}$ and $\bar{g}_{2\oplus}$ for ξ large are needed. This is dealt with in Appendix A while Appendix B treats the remaining terms of interest so that

$$\begin{aligned} p^l(x,+0) = {} & \rho U_0 C h^{-\frac{1}{2}}[(2\pi)^{-\frac{1}{2}}(AahU_0^{-1}b_0+b_{20})(x/h)^{-\frac{1}{2}} \\ & + AahU_0^{-1}(c_{10}-\mu_{20}-\lambda_{20})+\mu_{20}+\lambda_{20}+O(x/h)^{\frac{1}{2}}] \text{ as } x\rightarrow+0\,, \end{aligned} \tag{4.6a}$$

$$\begin{aligned} p^l(x,-0) = {} & -\rho U_0 C h^{-\frac{1}{2}}[(2\pi)^{-\frac{1}{2}}(AahU_0^{-1}b_0+b_{20})(x/h)^{-\frac{1}{2}} \\ & + AahU_0^{-1}(d_{10}-\mu_{20})+\mu_{20}+O(x/h)^{\frac{1}{2}}] \text{ as } x\rightarrow+0 \end{aligned} \tag{4.6b}$$

while

$$p^l(x,+0) = -\rho U_0 C h^{-\frac{1}{2}}[AahU_0^{-1}(c_{10}-\mu_{20}-\lambda_{20})+\mu_{20}+\lambda_{20}+O(|x|/h)^{\frac{1}{2}}] \text{ as } x\rightarrow-0\,, \tag{4.6c}$$

$$p^l(x,-0) = \rho U_0 C h^{-\frac{1}{2}}[AahU_0^{-1}(d_{10}-\mu_{20})+\mu_{20}+O(|x|/h)^{\frac{1}{2}}] \text{ as } x\rightarrow-0 \tag{4.6d}$$

where $b_0\ (=b_{10}-b_{20})$ is a function of a (see Fig. 4); the coefficients b_{20}, c_{10}, d_{10}, μ_{20} and λ_{20} are all defined in the appendices. [The contribution of the first term in the equation for $\bar{p}^l$ is contained in the $O|x|^{\frac{1}{2}}$ terms in the last two formulas.]

On the other hand direct expansion gives

$$p^\infty(x,\pm 0) = \rho U_0 C|x|^{-\frac{1}{2}} \text{ as } x\rightarrow-0\,, \tag{4.7a}$$

$$p^\infty(x,\pm 0) = \mp 2\rho A C x^{\frac{1}{2}} \text{ as } x\rightarrow+0\,. \tag{4.7b}$$

Since the pressure is continuous on the negative x-axis we must have

$$c_{10}+d_{10} = (1-a^{-\frac{1}{2}})a_0\;;\;\; \lambda_{20}+2\mu_{20} = a_0 \tag{4.8}$$

a result we were unable to prove directly.

To avoid the type of anomalous pressure behavior reported by Toomre and Rott, some care is needed in interpreting our results for p^r and p^l when taking the limit of remote bounding ($h\rightarrow\infty$ in Fig. 1). In our case we must keep Aah fixed less than U_0; otherwise there would be a reversal in the incident profile and boundary-layer theory would no longer be applicable. Furthermore, even in this limit infinite velocities are undesirable (*cf.* [7]), so Ah must also be kept finite.

As expected p_x^l swamps p_x^∞ on the plate near the leading edge; thus whenever there is local circulation at the leading edge the Li–Murray pressure gradient is relatively insignificant.

Ahead of the plate p^∞, which is independent of the shear is still dominant.

Taking into account both sides of the plate, the Li–Murray effect on lift is

$$\tfrac{8}{3}\rho A C x^{\frac{3}{2}}$$

for the first x units of the plate, whereas the lateral bounding (in this case due to the wall and uniform potential flow) gives two more important terms, namely

$$\begin{aligned}&-2^{\frac{3}{2}}\pi^{-\frac{1}{2}}\rho U_0 C(AahU_0^{-1}b_0+b_{20})x^{\frac{1}{2}}\\&-\rho U_0 Ch^{-\frac{1}{2}}[AahU_0^{-1}(c_{10}+d_{10}-2\mu_{20}-\lambda_{20})+2\mu_{20}+\lambda_{20}-AahU_0^{-1}a_0a^{-\frac{1}{2}}+a_0]x\\&=-2^{\frac{3}{2}}\pi^{-\frac{1}{2}}\rho U_0 C(AahU_0^{-1}b_0+b_{20})x^{\frac{1}{2}}-2\rho U_0 Ch^{-\frac{1}{2}}a_0(1-Aa^{\frac{1}{2}}hU_0^{-1})x\,.\end{aligned}\tag{4.9}$$

The importance of the inviscid pressure lies in its influence on the forces experienced by the plate. An $O(x^{\alpha-\frac{1}{2}})$ pressure behavior outside the boundary layer is associated with a second order shearing stress $O(x^{\alpha-1})$ on the plate. In our case the leading term in p^l therefore leads to a non-integrable shearing stress on either side of the plate; albeit since the stress is equal and opposite on the two sides at each x, there is cancellation and the total drag is zero. Then the next term in p^l and the leading term in p^r jointly provide the main drag contribution $O(x^{\frac{1}{2}})$; this being more important than the Li–Murray drag $O(x)$. Its domination in our case persists even when the bounding is symmetric.

It should be emphasized that the effects of the bounding on the lift and drag will, in general, depend on both the nature of the lateral bounding imposed as well as the degree of asymmetry. Only for strong bounding are such effects totally independent of the shear. While, as stated earlier, asymmetry in the bounding is sufficient for inducing local circulation, it is not a necessary condition. To be sure, local circulation can also be induced by arranging different lateral boundings on the two sides of the plate. In particular we observe that for the symmetric case ($a=1$, $b_{10}=0$), both terms in equation (4.9) survive.

The behavior of p^r and p^l far from the leading edge are best investigated by expanding their transforms near the singularity (in the appropriate half plane) closest to the strip of regularity. Conditions far upstream are determined by the highest singularity in the lower half plane. In $\bar{p}^r$, this occurs at $\xi=-i\varepsilon/h$ followed by poles at $\xi=-i\pi/h$ and at $\xi=-i\pi/ah$ for $\bar{p}^r(x,\pm 0)$ respectively. We then find

$$p^r(x,+0)=-\rho U_0 C|x|^{-\frac{1}{2}}+O(e^{\pi x/h})\quad\text{as }x\to-\infty\,,\tag{4.10a}$$

$$p^r(x,-0)=-\rho CAah|x|^{-\frac{1}{2}}+O(e^{\pi x/ah})\text{ as }x\to-\infty\,.\tag{4.10b}$$

The terms $\bar{g}_{1\oplus}|\xi|\coth|\xi|h$ and $\bar{g}_{1\oplus}|\xi|\coth a|\xi|h$ in $\bar{p}^l$ give exponentially small contributions, their highest singularity being at $\xi=-\pi i/(1+a)h$. We therefore focus attention on the remaining terms in $\bar{p}^l$. Each of these has its highest singularity at $\xi=-i\varepsilon/h$ where both $\bar{g}_{2\oplus}$ and $|\xi|$ have branch cuts. The asymptotic behavior of $\bar{g}_{2\oplus}$ near $\xi=0$ is treated in Appendix C.

We find

$$p^l(x,+0)=\rho Ch^{\frac{1}{2}}(U_0h^{-1}-A)(1-AahU_0^{-1})[(|x|/h)^{-\frac{1}{2}}+O(|x|/h)^{-\frac{3}{2}}]\text{ as }x\to-\infty\,,\tag{4.11a}$$

$$p^l(x,-0)=-\rho ACh^{\frac{1}{2}}(1-AahU_0^{-1})[(|x|/h)^{-\frac{1}{2}}+O(|x|/h)^{-\frac{3}{2}}]\text{ as }x\to-\infty\,.\tag{4.11b}$$

From (3.2) we find directly

$$p^\infty(x,0)=\rho U_0 C|x|^{-\frac{1}{2}}\text{ as }x\to-\infty\,.\tag{4.12}$$

For the case of strong bounding (*cf.* [7] and [8]), it was shown that while p^∞ and p^r+p^l separately have algebraic behavior, their sum has exponential decay; this curious cancellation is missing in our case since

$$p(x,0)\sim\rho U_0 C(1-AahU_0^{-1})(1-AhU_0^{-1})|x|^{-\frac{1}{2}}\text{ as }x\to-\infty\,.\tag{4.13}$$

Such algebraic behavior, typical of potential flow will always occur whenever the bounding is weak. Note that in the absence of shear (4.13) gives the correct result for the classical problem.

Conditions far downstream are determined by the lowest singularity in the upper half plane.

In $\bar{p}^r$ this occurs at $\xi=0$ where $\bar{n}_\ominus$ has a branch cut. Only $\bar{n}_\ominus|\xi|\coth|\xi|h$ and $\bar{n}_\ominus|\xi|\coth a|\xi|h$ contribute since the contribution from $\bar{n}_\ominus|\xi|(=O(\varepsilon^{\frac{1}{2}}))$ is zero in the limit.

Thus

$$p^r(x, +0) = -2\rho U_0 C h^{-\frac{1}{2}}(x/h)^{\frac{1}{2}}[1+O(h^2/x^2)] \text{ as } x\to\infty , \tag{4.14a}$$

$$p^r(x, -0) = -2\rho C A a^{\frac{1}{2}} h^{\frac{1}{2}}(x/ah)^{\frac{1}{2}}[1+O(a^2h^2/x^2)] \text{ as } x\to\infty . \tag{4.14b}$$

Since $\bar{g}_{1\oplus}$ and $\bar{g}_{2\oplus}$ have no singularities in the upper half plane, except for the branch cut for $\bar{g}_{2\oplus}|\xi|$ at $\xi=i\varepsilon/h$, the only other singularities are simple poles. $\bar{g}_{1\oplus}|\xi|\coth|\xi|h$ and $\bar{g}_{2\oplus}|\xi|$-$\coth|\xi|h$ have their lowest pole at $\xi=\pi i/h$ while that for $\bar{g}_{1\oplus}|\xi|\coth a|\xi|h$ lies at $\pi i/ah$. Expansion of $\bar{g}_{2\oplus}|\xi|$ around $\xi=0$ using the asymptotic expansion for $\bar{g}_{2\oplus}$ derived in Appendix C then gives

$$p^l(x, +0) = O(e^{-\pi x/h}) \text{ as } x\to\infty , \tag{4.15a}$$

$$p^l(x, -0) = -\rho U_0 C h^{-\frac{1}{2}}(1-AahU_0^{-1})\Big[(x/h)^{-\frac{3}{2}} - \frac{l_0}{\pi}(x/h)^{-2} + \frac{2l_0}{\pi^2}(x/h)^{-3}\log(x/h) + \gamma(x/h)^{-3} + O((x/h)^{-3}(1+\log(x/h)))^2 + \dots\Big] \text{ as } x\to\infty \tag{4.15b}$$

where

$$\gamma = \frac{2}{\pi^2}[(\log \vartheta_2\pi - \tfrac{1}{2} - \vartheta_2)l_0 - \pi l_1]$$

l_0, l_1 and ϑ_2 having been defined in Appendix C. Again, direct expansion gives

$$p^\infty(x, \pm 0) = \mp 2\rho A C x^{\frac{1}{2}} \text{ as } x\to\infty . \tag{4.16}$$

Far downstream the pressure gradient on either side of the plate tends to zero. For the lateral bounding considered by Toomre and Rott, the pressure gradient far downstream becomes vanishingly small compared with the Li–Murray value p_x^∞; since p^r+p^l provides cancellation for p^∞. However for the bounding considered in [7] no such cancellation was provided by their p^w (analogous to p^r+p^l). Since both forms of bounding are present in our case there is some interest in seeing how the behavior downstream is modified.

We indeed find that for symmetric bounding ($a=1$), $p_x(x, +0)$ calculated from equations (4.14)–(4.16) agrees with Ludford and Olunloyo's value: below the plate p_x^r provides cancellation for p_x^∞ thereby reproducing Toomre and Rott's result; the correction in either case being $O(x/h)^{-\frac{3}{2}}$ is relatively insignificant. Otherwise stated, the behavior of the pressure far downstream is more strongly influenced by the form of bounding than by discontinuities in the incident profile at the leading edge of the plate.

The log terms (*cf.* equation (4.15b)) which, for the first time, now appear in the inviscid pressure will induce corresponding terms in the boundary layer. It has been well known for some time that such log terms can arise in first order boundary layer solutions (see Van Dyke's 1964 treatment of the parabola in a uniform stream [13]) and in 3rd and higher orders boundary layers (Goldstein [14]). However, only recently (1972) has it been reported in the literature of second order boundary layer theory (see Kapila *et al.* [11]). Such log terms, since they are missing in [7] and [8] and only occur below the plate here, can only be associated with weak bounding.

We again find from equations (4.14)–(4.16) that the pressures above and below the plate are different so that a global circulation of $O(\nu^{\frac{1}{2}})$ is induced by equalizing them at some station downstream. Such a global circulation will now be considered in detail.

5. Induced global circulation

The global circulation can be found either by conformal transformation or by the Wiener–Hopf technique. We choose the latter partly for uniformity but chiefly because the detailed behavior of the circulation pressure p^c is more readily displayed.

The problem is to find a potential function Ψ^c which dies out as $y \to -\infty$ and takes on the boundary values

$$\Psi^c(x, h) \quad = 0\,, \tag{5.1a}$$

$$\Psi^c(x, \pm 0) = \begin{cases} g^c(x) & \text{for} \quad x < 0\,, \\ \psi_0 & \text{for} \quad x > 0 \end{cases} \tag{5.1b}$$

and

$$\Delta \Psi^c_y(x, 0) = \Psi^c_y(x, +0) - \Psi^c_y(x, -0) = \begin{cases} 0 & \text{for} \quad x < 0\,, \\ f(x) & \text{for} \quad x > 0 \end{cases} \tag{5.2}$$

where $g^c(x)$ and $f(x)$ are unknown. On taking the Fourier transform we immediately write

$$\overline{\Psi^c} = \begin{cases} (\bar{g}^c_\oplus + \bar{s}_\ominus)\dfrac{\sinh \xi(h-y)}{\sinh \xi h} & \text{for} \quad 0 \leqq y \leqq h\,, \\ (\bar{g}^c_\oplus + \bar{s}_\ominus)e^{|\xi| y} & \text{for} \quad y \leqq 0 \end{cases} \tag{5.3}$$

satisfying the boundary values (5.1).

Here

$$\bar{s}_\ominus = \psi_0 / i\xi$$

corresponding to

$$s(x) = \begin{cases} 0 & \text{for} \quad x < 0\,, \\ \psi_0 & \text{for} \quad x > 0\,. \end{cases}$$

The jump condition (5.2) now gives the Wiener–Hopf equation

$$K\bar{g}^c_\oplus + \bar{s}_\ominus h|\xi|(\coth|\xi|h+1) = -h\bar{f}_\ominus \tag{5.4}$$

where the kernel

$$K = h|\xi|(\coth|\xi|h+1)$$

is easily factorized as

$$K = K_{2\oplus}K_{2\ominus}\,.$$

[Note that $K_{2\oplus}$ and $K_{2\ominus}$ were defined in section 2.]

In the overlap strip $-\varepsilon/h < \text{Im}\,\xi < 0$ we can rewrite (5.4) as

$$\bar{g}^c_\oplus K_{2\oplus} - P^c_\oplus = P^c_\ominus - \frac{h\bar{f}_\ominus}{K_{2\ominus}} \tag{5.5}$$

where

$$P^c_\oplus = -\bar{s}_\ominus(K_{2\oplus}(\xi) - K_{2\oplus}(0)) = -\bar{s}_\ominus(K_{2\oplus} - 1)\,; \quad P^c_\ominus = -\bar{s}_\ominus$$

so that the left-hand side of (5.5) is regular in the upper half plane Im $\xi > -\varepsilon/h$ and the right-hand side is regular in the overlapping lower half plane Im $\xi < 0$. Together the two sides form an entire function which, in order to guarantee an integrable lift at the leading edge, must be set to zero.

Thus

$$\bar{g}^c_\oplus = \frac{P^c_\oplus}{K_{2\oplus}} = \bar{s}_\ominus\left(\frac{1}{K_{2\oplus}} - 1\right). \tag{5.6}$$

Substitution of $\bar{g}^c_\oplus$ into the formula (5.3) now gives the circulation streamfunction.

In particular, to find the asymptotic behavior of the circulation pressure p^c in different regimes of the x-axis we look at its transform

$$\bar{p}^c(\xi, \pm 0) = \begin{cases} \rho U_0(|\xi| \coth |\xi| h) \dfrac{\bar{s}_\ominus}{K_{2\oplus}} \\ -\rho U_0 \dfrac{\bar{s}_\ominus |\xi|}{K_{2\oplus}} \end{cases} + \rho A (\bar{g}^c_\oplus + \bar{s}_\ominus). \tag{5.7}$$

Following the procedure outlined in section 4, we find

$$p^c(x, \pm 0) = \rho U_0 \psi_0 h^{-1} [\pm \sigma (x/h)^{-\frac{1}{2}} + (\tilde{\omega} + Ah/U_0) + O(x/h)^{\frac{1}{2}}] \text{ as } x \to +0 \tag{5.8}$$

where

$$\sigma = -\frac{1}{2\pi\alpha_1^{\frac{1}{2}}}, \quad \tilde{\omega} = \frac{\alpha_2 - 1}{2\pi\alpha_1^2},$$

$$2\pi\alpha_1 = 3\pi\alpha_2 = 1 \tag{5.9}$$

and

$$p^c(x, 0) = \rho U_0 \psi_0 h^{-1} [\tilde{\omega} + Ah/U_0 + O(|x|/h)^{\frac{1}{2}}] \text{ as } x \to -0. \tag{5.10}$$

These formulas indicate that near the leading edge p^c behaves like p^l providing a lift

$$4\sigma\rho U_0 (x/h)^{\frac{1}{2}},$$

however unlike p^l it has no $O(x)$ lift term. The drag contribution, like in p^l is again $O(x)$.

For the behavior far ahead of the leading edge we obtain

$$p^c(x, +0) = \rho U_0 h^{-1} \psi_0 [h/\pi x + (1 - \vartheta_2) h^2/\pi^2 x^2 + O(h^3/x^3)] \text{ as } x \to -\infty \tag{5.11}$$

while far downstream we find

$$p^c(x, +0) = \rho\psi_0 [A + U_0 h^{-1} + O(e^{-\pi x/h})] \text{ as } x \to \infty, \tag{5.12a}$$

$$p^c(x, -0) = \rho\psi_0 [A + U_0 h^{-1} \{(\pi x/h)^{-1} + (\pi x/h)^{-2} \log (x/h) + \tilde{\gamma} (\pi x/h)^{-2} + O(x^{-2} \log x)^2 + \ldots\}] \text{ as } x \to \infty \tag{5.12b}$$

where $\tilde{\gamma} = (\log \vartheta_2 + \vartheta_2 - 2 - \log 2)$.

Here again log terms are present below the plate; in addition the x^{-1} term in the last formula induces a resonance that will be discussed in the next section.

We have so far avoided discussing the disposable constant ψ_0, the total flux anticlockwise around the plate. Different values for ψ_0 can be arranged but of main interest is its value when the total pressures above and below the plate are equalized at some station $x = x_\infty$ far downstream. From the results (4.14)–(4.16) and (5.12) we conclude

$$\psi_0 = 2\, U_0^{-1} C x_\infty^{\frac{1}{2}} [U_0 + Ah + O(x_\infty)^{-2}]$$

is the strength of the global circulation. It is not a function of a, reflecting its independence of the degree of asymmetry in the bounding.

6a. The second-order boundary layer near the leading edge

Li's original aim was to find the effect of free-stream vorticity on the shearing stress at the plate. To accomplish this the second-order boundary layer matching the disturbed inviscid flow must be determined. In [8] it was shown that it has three components, due to (i) the circulation; (ii) the walls [discussed years ago (1953) by Kuo [15] in a different context]; and (iii) the shear (Li–Murray). The first provides a non-integrable but cancelling drag from the top and bottom of the plate, the second $O(x^{\frac{1}{2}})$, and the third $O(x)$. Not only is the latter the least important but there is also cancellation along the whole length of the plate as can be seen *a priori*, so that the original question does not have much substance anyway!

A detailed discussion of these boundary layer solutions near the leading edge has been given in [8] and will not be repeated here. Instead we deduce that for our case the leading edge drag for the top of the plate is

$$-0.9962\,[\beta/2\,\{(\mu_{20}+\lambda_{20})(1-AahU_0^{-1})+a_0 \\ +AahU_0^{-1}c_{10}\}+\tilde{\omega}\bar{\psi}_0]\,R^{-1}\rho U_0^2 h^{\frac{1}{2}} x^{\frac{1}{2}} \tag{6.1a}$$

where

$$R = U_0 h/\nu \text{ (Reynolds Number)} ; \; \bar{\psi}_0 = R^{\frac{1}{2}}\psi_0/U_0 h$$

while for the bottom we obtain

$$-0.9962\,[\beta/2\,\{-\mu_{20}(1-AahU_0^{-1})+a_0 a^{-\frac{1}{2}}-d_{10}\}+\tilde{\omega}\bar{\psi}_0]\,R^{-1}\rho U_0^2 h^{\frac{1}{2}} x^{\frac{1}{2}} . \tag{6.1b}$$

The most important contribution (ignoring the Imai effect) to the leading edge drag then comes from summing the expressions (6.1a, b). While $\bar{\psi}_0$ depends on the station where the pressures are equalized downstream [$\tilde{\omega}$ being readily computed from (5.9)], the remaining coefficient

$$\lambda_{20}+a_0+AahU_0^{-1}(a_0 a^{-\frac{1}{2}}+\delta_0) \tag{6.2}$$

where

$$\delta_0 = (c_{10}-d_{10}-\lambda_{20})$$

depends on both the shear A, and the degree of asymmetry in the bounding. Fig. 4 displays δ_0 as a function of a. From this graph and the relations (4.8) and (B.1) the coefficients c_{10} and d_{10} which occur in (6.1) can be evaluated. Only in the presence of strong bounding is this coefficient independent of shear.

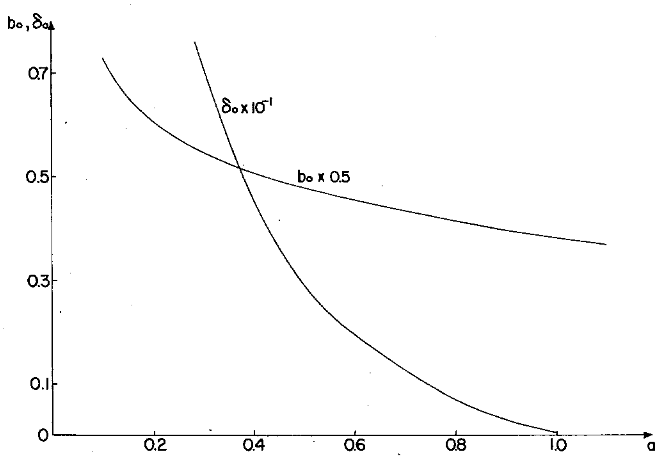

Figure 4. Variation of the coefficients b_0, δ_0 with the degree of geometrical asymmetry a in the bounding.

6b. The second-order boundary layer far downstream

We are interested in the boundary layer downstream only to the extent that it exhibits a new phenomenon. Accordingly, attention is restricted to the induced global circulation.

Referring velocities and lengths to U_0 and to h respectively and then using the non dimensionalized x and η as independent variables we can represent the streamfunction in the boundary layer far downstream as

$$\Psi = R^{-\frac{1}{2}}[x^{\frac{1}{2}} f_0(\eta)+\bar{\psi}_0+R^{-\frac{1}{2}} g(x,\eta)+\ldots]$$

where

$$Y = R^{\frac{1}{2}} y ; \quad \eta = Y/2x^{\frac{1}{2}}$$

and f_0 is the Blasius function. On retaining terms up to $O(R^{-1})$ we obtain for $g(x,\eta)$

$$g_{\eta\eta\eta\eta}+f_0 g_{\eta\eta\eta}+2f_0' g_{\eta\eta}+f_0'' g_\eta-2x(f_0' g_{\eta\eta x}-f_0''' g_x)=0 \tag{6.3}$$

with

$$g(0)=g_\eta(0)=0 ; \quad g_\eta = F(x,0)+\text{a.e.s. in } \eta \text{ as } \eta\to\infty$$

where the forcing function

$$F(x,0)=2x^{\frac{1}{2}}\bar{\psi}_y(x,0)$$

and $\bar{\psi}_y(x,0)$ is the non-dimensionalized disturbance velocity.

Since the boundary layer must match the inviscid flow outside it, the form assumed for $g(x,\eta)$ thereby depends on $F(x,0)$.

Above the plate we find

$$F(x,+0)=-2\bar{\psi}_0 x^{\frac{1}{2}}+\text{a.e.s.} \tag{6.4}$$

and for its associated boundary layer we write

$$g(x,\eta)=E_1x^{\alpha}f_1(\eta)+\sum_{\lambda} D_\lambda x^\lambda G_\lambda(\eta)\,. \tag{6.5}$$

Here the first term in (6.5) is found by direct matching with (6.4) while the second consists of the eigensolutions (λ being the eigenvalue and G_λ the corresponding eigenfunction) satisfying the differential equation

$$L_\lambda(G_\lambda)=0 \tag{6.6}$$

with

$$G_\lambda(0)=G'_\lambda(0)=0\,;\quad G'_\lambda=\text{a.e.s. in } \eta \quad \text{as} \quad \eta\to\infty\,.$$

The operator

$$L_\lambda\equiv\frac{d}{d\eta}\left\{\frac{d^3}{d\eta^3}+f_0\frac{d^2}{d\eta^2}+(1-2\lambda)f'_0\frac{d}{d\eta}+2\lambda f''_0\right\}$$

but E_1 and D_λ are arbitrary constants. Libby and Fox [10] in treating the above problem have shown that the eigenvalues are all negative and form a countable set the first few being $-\frac{1}{2}$, -1.387, -2.314, -3.5, -4.24 ... . Unlike E_1, the D_λ cannot be found by direct matching but instead depend on the global character of $F(x,0)$ (see Wilson [16]).

For this case we find

$$E_1=-\bar{\psi}_0\,;\quad \alpha=\tfrac{1}{2}$$

so that the leading term in the boundary layer expansion is the $O(x^{\frac{1}{2}})$ forcing function followed by the $O(x^{-\frac{1}{2}})$ eigensolution, the remaining eigensolutions following in order.

Below the plate a curious resonance is induced in the boundary layer. This is because

$$F(x,-0)=-2\pi\bar{\psi}_0[x^{-\frac{1}{2}}+x^{-\frac{3}{2}}\log x+\tilde{\gamma}x^{-\frac{3}{2}}+O(x^{-\frac{5}{2}}\log^2 x)]$$

has as its leading term, $x^{-\frac{1}{2}}$ whose exponent coincides with the first eigenvalue ($\lambda=-\frac{1}{2}$) in the boundary layer eigensolutions. Our $g(x,\eta)$ must then assume the form

$$g(x,\eta)=-2\pi\bar{\psi}_0[x^{-\frac{1}{2}}H_1(\eta)+D_{-\frac{1}{2}}x^{-\frac{1}{2}}\log xG_{-\frac{1}{2}}(\eta)$$
$$+D_{-1.387}x^{-1.387}G_{-1.387}(\eta)+E_2x^{-\frac{3}{2}}\log xf_2(\eta)+\ldots] \tag{6.7}$$

which when substituted into (6.3) yields

$$L_{-\frac{1}{2}}(G_{-\frac{1}{2}}(\eta))=0$$

as the governing equation for $G_{-\frac{1}{2}}(\eta)$ with

$$G_{-\frac{1}{2}}(0)=G'_{-\frac{1}{2}}(0)=0\,;\quad G'_{-\frac{1}{2}}=\text{a.e.s. in } \eta \quad \text{as} \quad \eta\to\infty$$

and

$$L_{-\frac{1}{2}}(H_1(\eta))=2(f'_0G''_{-\frac{1}{2}}-f'''_0G_{-\frac{1}{2}}) \tag{6.8}$$

with

$$H_1(0)=H'_1(0)=0\,;\quad H'_1=1+\text{a.e.s. as } \eta\to\infty\,.$$

The solution for $G_{-\frac{1}{2}}(\eta)$ was discussed years ago (1948) in a different context by Alden [17]. To be sure

$$G_{-\frac{1}{2}}(\eta) = A_2(\eta f_0' - f_0)$$

where A_2 is an arbitrary constant to be determined consistent with (6.8). This is easily done by invoking a modified version of a trick originally attributed to Devan (see Van Dyke [13]). For our case $A_2 = -0.85$.

Here again the E_n are found by direct matching with $F(x, 0^-)$ whereas the D_λ cannot be found without investigating a region $O(R^{-1})$ at the leading edge of the plate.

Such resonance as found here is suppressed by the presence of walls: it is independent of shear and persists as the bounding recedes. In fact it can be shown to be present in the Li–Murray case by (realistically) admitting induced global circulations.

Appendix A: Asymptotic behavior of $\bar{g}_{1\oplus}$ and $\bar{g}_{2\oplus}$ for ξ large

Some terms in p^l involve $g_2(x)$, whose asymptotic behavior as $x \to O^-$ is determined by that of its transform as $\xi \to \infty$.

The transform is given by the result

$$\bar{g}_{2\oplus} = P_{2\oplus}/K_{2\oplus}$$

where $P_{2\oplus}$ and $K_{2\oplus}$ are given by equations (2.14) and (2.16) respectively. Because of the exponential convergence at $z = \pm\infty$, the asymptotic expansion of $P_{2\oplus}$ can be obtained by writing

$$(z-\xi)^{-1} = -(1 + z/\xi + z^2/\xi^2 + \ldots)/\xi$$

in its integrand and integrating term by term. Thus

$$P_{2\oplus}(\xi) \sim -\frac{1}{i\xi}\{b_{20} + b_{21}/h\xi + b_{22}/h^2\xi^2 + \ldots\}$$

where the coefficients

$$b_{2n} = \frac{h^{n+1}}{2\pi}\oint \frac{\bar{n}_\ominus(z)|z|z^n(\coth|z|h - 1)}{K_{2\ominus}(z)}\, dz \tag{A.1}$$

are easily seen to be independent of h. They can be evaluated numerically by integrating along the real axis (after subtracting the $z^{-\frac{3}{2}}$ singularity at the origin in the case of b_{20}).

The asymptotic behavior of $K_{2\oplus}$ follows from Stirling's formula namely

$$K_{2\oplus}(\xi) = -(-2i\xi h)^{\frac{1}{2}}(1 + O(1/\xi)),$$

we therefore find

$$\bar{g}_{2\oplus} = [i\xi(-2i\xi h)^{\frac{1}{2}}]^{-1}(b_{20} + O(1/\xi)). \tag{A.2}$$

By following the same procedure we can write

$$P_{1\oplus}(\xi) \sim -\frac{1}{i\xi}\{b_{10} + b_{11}/h\xi + b_{12}/h^2\xi^2 + \ldots\}$$

where

$$b_{1n} = \frac{h^{n+1}}{2\pi}\oint \frac{\bar{n}_\ominus(z)z^{n+1}\sinh z(1-a)h}{K_{1\ominus}(z)\sinh zh \sinh azh}\, dz \tag{A.3}$$

so that for large ξ

$$\bar{g}_{1\oplus} = [i\xi(-2i\xi h)^{\frac{1}{2}}]^{-1}(b_{10} + O(1/\xi)). \tag{A.4}$$

The b_{1n} are functions of a, the degree asymmetry whereas the b_{2n} are constants (for example $b_{20} = -0.760$). The importance of b_{10} and b_{20} is to be found in their contribution towards the leading edge lift (*cf.* eq. 4.9).

From the above results for $\bar{g}_{1\oplus}$ and $\bar{g}_{2\oplus}$ we deduce that their contribution through the first term in eqs. (3.4a, b) for p^l is zero on the plate and is $O(|x|^{\frac{1}{2}})$ ahead of the plate as was noted under equation (4.6).

Appendix B: Asymptotic behavior of the $\oplus$ parts of terms like $\bar{g}_{2\oplus}|\xi|$ coth $|\xi|$ h in $\bar{p}^t$ for large ξ

The asymptotic behaviors of the integrals in equations (3.4) as $x \to \pm 0$ are determined by those of the $\oplus$ parts of their transforms as $\xi \to \infty$.

We can illustrate the results by considering

$$\bar{g}_{2\oplus}|\xi| \coth|\xi| h = F = F_1 + F_2$$

where

$$F_1 = \bar{g}_{2\oplus}|\xi|(\coth|\xi|h - 1)\,; \quad F_2 = \bar{g}_{2\oplus}|\xi|\,.$$

Following the decomposition theorem (Noble [12, p. 13])

$$F_1 = F_{1\oplus} + F_{1\ominus}$$

with

$$F_{1\oplus} = \pm \frac{1}{2\pi i} \oint_{-\infty}^{\infty} \frac{\bar{g}_{2\oplus}(z)|z|(\coth|z|h - 1)}{z - \xi}\, dz\,.$$

We can exploit the exponential convergence provided by $(\coth|z|h - 1)$ so that for large ξ we obtain

$$F_{1\oplus} = \mp \frac{1}{i\xi h}(\lambda_{20} + \lambda_{21}/\xi h + \lambda_{22}/\xi^2 h^2 + \ldots)$$

where the coefficients

$$\lambda_{2n} = \frac{h^{n+1}}{2\pi} \oint_{-\infty}^{\infty} \bar{g}_{2\oplus}(z)|z| z^n (\coth|z|h - 1)\, dz$$

are easily checked to be constants independent of h. In particular

$$\lambda_{20} = -0.175\,. \tag{B.1}$$

Next we write F_2 as the sum of a $\oplus$ and a $\ominus$ function with

$$F_{2\ominus} = -\frac{1}{2\pi i} \lim_{\varepsilon \to 0} \left[\oint_{-\infty}^{\infty} \frac{(\bar{g}_{2\oplus}(z) - g_{2\infty})|z|}{z - \xi}\, dz + \oint_{-\infty}^{\infty} \frac{g_{2\infty}|z|}{z - \xi}\, dz \right].$$

Here

$$g_{2\infty}(z) = \frac{b_{20}}{i(-2ih)^{\frac{1}{2}}(z + i\varepsilon/h)^{\frac{3}{2}}}$$

is the leading term in the asymptotic expansion of $\bar{g}_{2\oplus}(z)$ given in (A.2). Completing the contour in the lower half plane gives

$$-\frac{1}{2\pi i} \lim_{\varepsilon \to 0} \int_{-\infty}^{\infty} \frac{g_{2\infty}(z)|z|}{z - \xi}\, dz = \left(\frac{b_{20}}{i(-2ih\xi)^{\frac{1}{2}}} \right)_{\ominus}. \tag{B.2}$$

The remaining integral in $F_{2\ominus}$ can be rewritten as

$$\frac{1}{2\pi i} \lim_{\varepsilon \to 0} \left[\frac{1}{\xi} \int_{-\infty}^{\infty} |z|(\bar{g}_{2\oplus}(z) - g_{2\infty})dz - \frac{1}{\xi} \int_{-\infty}^{\infty} \frac{|z|(\bar{g}_{2\oplus} - g_{2\infty})}{z - \xi}\, z\, dz \right].$$

Both of these integrals are convergent since

$$g_{2\oplus}(z) - g_{2\infty} = O(z^{-\frac{5}{2}}) \text{ as } z \to \infty$$

so that

$$-\frac{1}{2\pi i} \int_{-\infty}^{\infty} \frac{(g_{2\oplus} - g_{2\infty})|z|}{z - \xi}\, dz = \frac{\mu_{20}}{i\xi h} + O(\xi^{-\frac{3}{2}})$$

where

$$\mu_{20} = \frac{h}{2\pi} \int_{-\infty}^{\infty} |z|(g_{2\oplus}(z) - g_{2\infty})dz\,. \tag{B.3}$$

Accordingly,

$$F_{2\ominus} = \frac{b_{20}}{i(-2i\xi h)^{\frac{1}{2}}} + \frac{\mu_{20}}{i\xi h} + O(\xi^{-\frac{3}{2}}). \tag{B.4}$$

The function $F_{2\oplus}$ can be treated the same way; the only difference is that the integral (B.2) is now zero since the point ξ now lies in the upper half plane. Thus

$$F_{2\oplus} = -\frac{\mu_{20}}{i\xi h} + O(\xi^{-2}). \tag{B.5}$$

Hence if we write

$$\bar{g}_{2\oplus}|\xi| \coth|\xi| h = F_{\oplus} + F_{\ominus}$$

then

$$F_{\ominus} = \frac{b_{20}}{i(-2i\xi h)^{\frac{1}{2}}} + \frac{\lambda_{20}+\mu_{20}}{i\xi h} + O(\xi^{-\frac{3}{2}}) \tag{B.6}$$

and

$$F_{\oplus} = -\frac{\lambda_{20}+\mu_{20}}{i\xi h} + O(\xi^{-2}). \tag{B.7}$$

Similarly we can write

$$\bar{g}_{1\oplus}|\xi| \coth|\xi| h = G_{\oplus} + G_{\ominus}$$

where

$$G_{\ominus} = \frac{b_{10}}{i(-2i\xi h)^{\frac{1}{2}}} + \frac{c_{10}}{i\xi h} + O(\xi^{-\frac{3}{2}}) \tag{B.8}$$

and

$$G_{\oplus} = -\frac{c_{10}}{i\xi h} + O(\xi^{-2}). \tag{B.9}$$

Here

$$c_{10} = \gamma_0 + \bar{c}_0,$$

$$\bar{c}_0 = \frac{h}{2\pi} \lim_{\varepsilon \to 0} \int_{-\infty}^{\infty} \bar{g}_{1\oplus}(z)|z|(\coth|z|h - 1)dz, \tag{B.10}$$

and

$$\gamma_0 = \frac{h}{2\pi} \int_{-\infty}^{\infty} |z| \left(\bar{g}_{1\oplus}(z) - \frac{b_{10}}{i(-2ih)^{\frac{1}{2}} \xi^{\frac{3}{2}}} \right) dz. \tag{B.11}$$

Finally we write

$$\bar{g}_{1\oplus}|\xi| \coth a|\xi| h = R_{\oplus} + R_{\ominus}$$

where

$$R_{\ominus} = \frac{b_{10}}{i(-2i\xi h)^{\frac{1}{2}}} + \frac{d_{10}}{i\xi h} + O(\xi^{-\frac{3}{2}}) \tag{B.12}$$

and

$$R_{\oplus} = -\frac{d_{10}}{i\xi h} + O(\xi^{-2}) \tag{B.13}$$

with

$$d_{10} = \bar{d}_0 + \gamma_0$$

and

$$\bar{d}_0 = \frac{h}{2\pi} \lim_{\varepsilon \to 0} \int_{-\infty}^{\infty} \bar{g}_{1\oplus}(z)|z|(\coth a|z|h - 1)dz \tag{B.14}$$

is, like $\bar{c}_0$, a function of a.

Inversion of the results (B.4–14) now gives the formulas (4.6).

Appendix C: Asymptotic behavior of $\bar{g}_{2\oplus}$ for small ξ

When Im $\xi \ll 1$, the integral $P_{2\oplus}$ (2.14) involved in $\bar{g}_{2\oplus}$ can be written as

$$P_{2\oplus} = \frac{h}{2\pi i}\left[\oint_{-\infty}^{\xi-\varepsilon/2h} \frac{\bar{n}_\ominus(z)|z|(\coth|z|h-1)}{K_{2\ominus}(z)(z-\xi)}dz + \int_{\xi+\varepsilon/2h}^{\infty} \frac{\bar{n}_\ominus(z)|z|(\coth|z|h-1)}{K_{2\ominus}(z)(z-\xi)}dz + \pi i\frac{\bar{n}_\ominus(\xi)|\xi|(\coth|\xi|h-1)}{K_{2\ominus}(\xi)}\right] \quad (C.1)$$

where the path of integration has been deformed onto the real axis indented both at the origin and in the neighborhood of the point ξ.

To obtain tractable integrals we rewrite the integrals in (C.1) as

$$\frac{h}{2\pi i}\left[\oint_{-\infty}^{\xi-\varepsilon/2h} \frac{\bar{n}_\ominus(z)}{z-\xi}\left\{\frac{|z|(\coth|z|h-1)}{K_{2\ominus}(z)} - \frac{A_m(z)}{K^0(z)}\right\}dz + \int_{\xi+\varepsilon/2h}^{\infty} \frac{\bar{n}_\ominus(z)}{z-\xi}\left\{\frac{|z|(\coth|z|h-1)}{K_{2\ominus}(z)} - \frac{A_m(z)}{K^0(z)}\right\}dz + \int_{-\infty}^{\xi-\varepsilon/2h}\frac{\bar{n}_\ominus(z)A_m(z)}{K^0(z)}dz + \int_{\xi+\varepsilon/2h}^{\infty}\frac{\bar{n}_\ominus(z)A_m(z)}{K^0(z)}dz\right] \quad (C.2)$$

where $A_m(z)$ is the first $m+1$ terms in the asymptotic expansion of z coth zh for small z and $K^0(z)$ is the asymptotic expansion for $K_{2\ominus}(z)$ for z small.

In the limit $\xi\to 0$; the first two integrals in (C.2) now combine to give

$$\frac{h}{2\pi}\oint_{-\infty}^{\infty}\frac{\bar{n}_\ominus(z)}{z-\xi}\left\{\frac{|z|(\coth|z|h-1)}{K_{2\ominus}(z)} - \frac{A_m(z)}{K^0(z)}\right\}dz \quad (C.3)$$

which has the asymptotic expansion

$$h[l_0+l_1(-i\xi h)+l_2(-i\xi h)^2+\ldots] \quad (C.4)$$

where

$$l_n = \frac{(-ih)^{-n}}{2\pi}\lim_{\varepsilon\to 0}\int_{-\infty}^{\infty}\frac{\bar{n}_\ominus(z)}{z^{n+1}}\left\{\frac{|z|(\coth|z|h-1)}{K_{2\ominus}(z)} - \frac{A_m(z)}{K^0(z)}\right\}dz\,. \quad (C.5)$$

The series (C.4) is obtained by writing

$$(z-\xi)^{-1} = (1+\xi/z+\xi^2/z^2+\ldots)/z$$

in the integrand in (C.3) and integrating term by term.

On the other hand, completing the contour in the lower half plane shows that the last two integrals in (C.2)

$$\int_{-\infty}^{\xi-\varepsilon/2h}\frac{\bar{n}_\ominus(z)A_m(z)}{K^0(z)(z-\xi)}dz + \int_{\xi+\varepsilon/2h}^{\infty}\frac{\bar{n}_\ominus(z)A_m(z)}{K^0(z)(z-\xi)}dz = -\pi i\left[\frac{\bar{n}_\ominus(\xi)A_m(\xi)}{K^0(\xi)}\right]$$

so that as $\xi\to 0$

$$\bar{g}_{2\oplus} \sim h\bar{n}_\ominus(\xi)\{|\xi|+\xi\coth\xi h - A_m(\xi)\} + hK_\oplus^{0^{-1}}(\xi)\sum_{n=0}^{\infty} l_n(-i\xi h)^n \quad (C.6)$$

where

$$K_\oplus^{0^{-1}} = \left[1+\sum_{k=2}^{\infty}\vartheta_k\left(-\frac{i\xi h}{\pi}\right)^{k-1}\right]\sum_{p=0}^{\infty}\frac{(-1)^p}{p!}\times$$
$$\times\left\{\frac{(\xi^2+\varepsilon^2/h^2)^{\frac{1}{2}}}{\pi}\left(\frac{\pi}{2}+i\log h\left[\frac{\xi+(\xi^2+\varepsilon^2/h^2)^{\frac{1}{2}}}{\varepsilon}\right]\right) - \frac{i\xi h}{\pi}\left(1-\log\frac{\varepsilon}{2\pi}\right)\right\}^p$$

is the asymptotic expansion for $(1/K_{2\oplus}(\xi))$ for small ξ. Here, ϑ_k which is tabulated (Abramowitz and Stegun [18 p. 256]) comes from writing

$$\frac{1}{\Gamma\left(1-\dfrac{i\xi h}{\pi}\right)} = 1 + \sum_{k=2}^{\infty} \vartheta_k \left(-\frac{i\xi h}{\pi}\right)^k \quad \text{for} \quad \text{small } \xi .$$

In contrast $\bar{g}_{1\oplus}$ gives no difficulty near $\xi = 0$ since it is regular there. This is because a series representation for $P_{1\oplus}$ can be found by completing the contour for the integral (2.11) in the lower half plane.

Acknowledgement

This research was supported in part by the U. S. Army Research Office–Durham and in part by the National Science Foundation under grant GP-28483 at Cornell University. The author is indebted to the thought-provoking discussions and suggestions provided by Mr. A. K. Kapila and Professor G. S. S. Ludford in the course of this investigation.

REFERENCES

[1] T. Y. Li, Effects of free-stream vorticity on the behavior of a viscous boundary layer, *J. Aero. Sci.*, 23 (1956) 1128–1129.
[2] J. D. Murray, The boundary layer on a flat plate in a stream with uniform shear, *J. Fluid Mech.*, 11 (1961) 309–316.
[3] M. B. Glauert, The pressure gradient induced by shear flow past a flat plate, *J. Aero. Sci.*, 29 (1962) 540–542.
[4] A. Toomre and N. Rott, On the pressure induced by the boundary layer on a flat plate in shear flow, *J. Fluid Mech.*, 19 (1964) 1–10.
[5] M. Van Dyke, Higher-order boundary-layer theory, *Annual Review of Fluid Mechanics*, 1 (1969) 265–291.
[6] W. Koch, G. S. S. Ludford and A. R. Seebass, Diffusion in shear flow past a semi-infinite flat plate; Part II; Viscous Effects, *Acta Mech.*, 12 (1971) 99–120.
[7] G. S. S. Ludford and V. O. S. Olunloyo, The forces on a flat plate in a Couette flow, *ZAMP*, 23 (1972) 115–124.
[8] G. S. S. Ludford and V. O. S. Olunloyo, Further results concerning the forces of a flat plate in a Couette flow, To appear in *ZAMP*.
[9] S. Goldstein, Some recent work on laminar boundary layers, *Developments in Mechanics, Vol. 2, Part I Fluid Mechanics*, 205 (1965). [Proc. 8th Midwestern Mechanics Conference, Cleveland 1963. New York; Pergamon Press.]
[10] P. A. Libby and H. Fox, Some perturbation solution in laminar boundary-layer theory. Part I, the momentum equation, *J. Fluid Mech.*, 17 (1963) 433–449.
[11] A. K. Kapila, G. S. S. Ludford and V. O. S. Olunloyo, Entry flow in a channel. Part 3: Inlet in a uniform stream, To appear in J. Fluid Mech.
[12] B. Noble, *Methods based on the Wiener–Hopf technique for the solution of Partial Differential Equations*, Pergamon Press (1958).
[13] M. Van Dyke, Higher approximations in boundary-layer theory. Part 3. Parabola in a uniform stream, *J. Fluid Mech.*, 19 (1964) 145–159.
[14] S. Goldstein, *Lectures on Fluid Mechanics*, Interscience (1960).
[15] Y. H. Kuo, On the flow of an incompressible viscous fluid past a flat plate at moderate Reynolds numbers, *J. Math. Phys.*, 32 (1953) 83–101.
[16] S. D. R. Wilson, Entry flow in a channel. Part 2. *J. Fluid Mech.*, 46 (1971) 787–799.
[17] H. L. Alden, Second approximation to the laminar boundary-layer flow over a flat plate, *J. Math. Phys.*, 27 (1948) 91–104.
[18] M. Abramowitz and I. A. Stegun, *Handbook of Mathematical functions.* Dover Publications, New York (1965).